

Characteristics of a tungsten film electrodeposited in a $\text{KF-B}_2\text{O}_3\text{-WO}_3$ melt and preparation of W–Cu–W three-layered films for heat sink application

Koji Nitta · Toshiyuki Nohira · Rika Hagiwara · Masatoshi Majima · Shinji Inazawa

Received: 13 July 2009 / Accepted: 27 March 2010 / Published online: 10 April 2010
© Springer Science+Business Media B.V. 2010

Abstract A tungsten film of 13 μm in thickness was obtained on a copper substrate by galvanostatic electrolysis at 30 mA cm^{-2} for 40 min in a $\text{KF-B}_2\text{O}_3\text{-WO}_3$ (67:26:7 mol%) melt at 850 °C. By cross-sectional scanning electron microscopy observation and energy dispersive X-ray analysis, the tungsten layer was found to be compact and free from cracks, voids and melt inclusion. The X-ray diffractometry analysis revealed that the phase was α -tungsten, and that (222) plane was significantly oriented parallel to the substrate. By nanoindentation, its hardness was found to be 8.4 GPa, which was larger than that of single crystal tungsten. Its Young's modulus was measured to be 410 GPa, which was similar with the reported value of single crystal tungsten. Its coefficient of linear thermal expansion and thermal conductivity were $4.5 \times 10^{-6} \text{ K}^{-1}$ and $178 \text{ W m}^{-1} \text{ K}^{-1}$, respectively, which were similar values for the tungsten produced by a conventional powder metallurgy method. Finally, W–Cu–W three-layered films were prepared for a heat sink application. It was confirmed that a three-layered film having a desired coefficient of linear thermal expansion can be prepared easily by this new molten salt method.

Keywords Tungsten · Molten salt · Electrodeposition · Linear thermal expansion

1 Introduction

Tungsten metal has the highest melting point (3,660 °C) among metals and has excellent properties such as good heat resistance, high strength and low thermal expansion. Thus, tungsten is used for a number of applications such as a contact probe pin for LSI testing [1], an electrode for cold cathode emission [2], a thermally conductive layer for heat sink [3], and an electrode for electric discharge machining [4]. However, the processing of tungsten is difficult because of its high hardness and brittleness. So, the commercially available products of tungsten are produced by powder metallurgy, which limits the shapes to simple ones like plate, wire and rod, and also makes the products expensive. Thus, applications of tungsten have been rather limited so far in spite of its excellent properties. If it is possible to plate a desired amount of tungsten at a desired place by electrodeposition, tungsten is expected to be used more widely. Although the electrodeposition of tungsten from an aqueous solution is extremely difficult, the electrodeposition from molten salt has been reported. Senderoff et al. [5, 6] obtained tungsten from alkali metal fluoride melts at 700–850 °C. Koyama et al. [7] successfully electrodeposited a tungsten film of 100 μm in thickness from a $\text{KF-B}_2\text{O}_3\text{-WO}_3$ melt at 850 °C. At lower temperatures of 350–450 °C, Katagiri et al. [8] succeeded in electrodepositing tungsten from $\text{ZnBr}_2\text{-NaBr}$ and $\text{ZnCl}_2\text{-NaCl}$ [9] melts. At further lower temperature of 250 °C, we reported the electrodeposition of tungsten from a $\text{ZnCl}_2\text{-NaCl-KCl}$ melt [10].

For the practical use of such electrodeposited tungsten, it is important to know its characteristics. For surface coating,

K. Nitta (✉) · T. Nohira · R. Hagiwara
Department of Fundamental Energy Science, Graduate School
of Energy Science, Kyoto University, Sakyo-ku,
Kyoto 606-8501, Japan
e-mail: nitta-koji@sei.co.jp

T. Nohira
e-mail: nohira@energy.kyoto-u.ac.jp

K. Nitta · M. Majima · S. Inazawa
Electronics and Materials R&D Labs, Sumitomo Electric
Industries, Ltd, 1-1-3, Shimaya, Konohana-ku,
Osaka 554-0024, Japan

for example, hardness is very important to increase wear resistance. Recently, the Cu/W composite materials are attracting attention as a heat sink material for high-power solid-state lasers [11, 12]. Although copper has a high thermal conductivity, its large coefficient of thermal expansion generates large thermal stress with the solid laser materials. Since tungsten has low thermal expansion, it is possible to prepare a heat conductor with a desired thermal expansion by combining copper and tungsten. A high Young's modulus of tungsten plays an important role in increasing the mechanical strength of the composite material in spite of the mismatch of thermal expansion between copper and tungsten. According to a theory of composite material [13], a copper ratio can be increased for a multilayer material compared with a dispersion material. For example, the same coefficients of linear thermal expansion are obtained for a multilayer material of W:Cu = 60:40 vol% and a dispersion material of W:Cu = 70:30 vol%, which means the multilayer has a higher thermal conductivity. For a thermally conductive layer for a heat sink, the total thickness is desired to be between 50 and 100 μm to attain both high thermal conductivity and high mechanical strength. However, it is very difficult to prepare such a thin W–Cu multilayer by a conventional powder metallurgy method. On the other hand, a thin film of tungsten can be electrodeposited on a copper substrate.

From this background, in this study, tungsten films were electrodeposited on a copper substrate in a $\text{KF–B}_2\text{O}_3\text{–WO}_3$ melt at 850 °C. Firstly, the morphology and impurities were studied for the tungsten layer by SEM and EDX. Secondly, the phase and crystal orientation were examined by XRD. Since the thermal conductivity, the coefficient of linear thermal expansion and the Young's modulus are of importance for a heat sink application, these properties were measured for the tungsten layer after removing the copper substrate. So far, these properties have not been reported for the electrodeposited tungsten films. Finally, W–Cu–W three-layered films with different Cu/W ratios were prepared and evaluated. Their coefficients of linear thermal expansion were measured and compared with the values predicted by the theory of composite material.

2 Experimental

2.1 Chemicals

All the chemicals were anhydrous reagent grade. The composition of molten salt was 67 mol% KF (99%, Wako Pure Chemical Industries, Ltd.), 26 mol% B_2O_3 (99%, Wako Pure Chemical Industries, Ltd.) and 7 mol% WO_3 (99%, Mitsui Chemicals Co., Ltd.), and total weight was 600 g. The mixture was put in a SiC crucible (Tokai

Konetsu Kogyo Co., Ltd., RS420) and dried under vacuum at 500 °C for a day.

2.2 Electrodeposition and cyclic voltammetry

The electrochemical measurements were carried out in the apparatus shown in Fig. 1 under argon flow. For the electrodeposition experiments, the working electrode was a copper film (99.9%, $20 \times 40 \times 0.05$ mm or $20 \times 40 \times 0.02$ mm, Nilaco Corp.) and the counter electrode was a tungsten plate (99.95%, $10 \times 50 \times 1$ mm, Nilaco Corp.). Before the electrochemical measurement, for the purpose of purification, preelectrolysis was carried out at 850 °C at 100 mA cm^{-2} over 2 h, using a molybdenum plate (99.9%, $20 \times 50 \times 0.1$ mm, Nilaco Corp.) as the cathode and a tungsten plate ($10 \times 50 \times 1$ mm) as the anode. The electrodeposition was carried out at a constant current density of 30 mA cm^{-2} . After the electrodeposition, the obtained sample was immersed in distilled water to remove the salts. The cyclic voltammetry was carried out using a tungsten wire (99.95%, 1 mm in diameter, Nilaco Corp.) immersed in the melt as the reference electrode. The working electrode was a copper film or the tungsten electrodeposited on a copper film. The counter electrode was a tungsten plate.

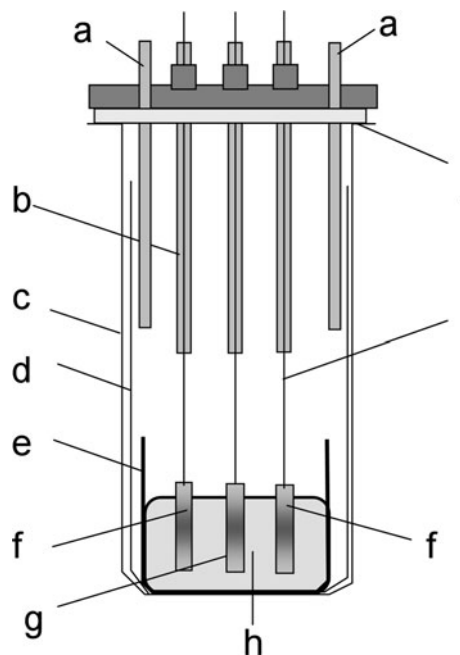


Fig. 1 Schematic drawing of apparatus of electrolysis. *a*: Ar inlet or outlet, *b*: alumina tube, *c*: outer silica vessel, *d*: inner silica vessel, *e*: SiC crucible, *f*: counter electrode (W), *g*: working electrode (Cu), *h*: bath (67 mol% KF—26 mol% B_2O_3 —7 mol% WO_3 melt), *i*: Mo wire, *j*: PTFE gasket

2.3 Characterization and property measurement of the electrodeposits

The deposits on a copper substrate were characterized by scanning electron microscopy (SEM, Hitachi Ltd., S-2600-H and Zeiss, Ultra55), energy dispersive X-ray analysis (EDX, edax, S-UTW) and X-ray diffractometry (XRD, Rigaku Corp., Multi Flex). The hardness and the Young's modulus of the deposits were measured by nanoindentation [14] (Nanoindenter, MTS System Corp., G200). This system was installed a Berkovich indenter and had load and displacement resolutions of 50 nN and 0.1 nm. The sample was mounted in epoxy resin and the face for measurement was exposed by mirror polishing. The measurement was carried out at 10 points in 20 μm pitch and 300 nm depth. For the measurements of the coefficient of linear thermal expansion and the thermal conductivity, the tungsten film was separated from a copper substrate by chemical dissolution of copper in a dilute nitric acid solution. The coefficient of linear thermal expansion was measured by the laser speckle technique (Laser speckle distortion sensor, Hamamatsu photonics, C4240-02) from 50 to 200 $^{\circ}\text{C}$ at a heating rate of 10 $^{\circ}\text{C min}^{-1}$. The thermal conductivity was calculated from the thermal effusivity, which was measured by the thermoreflectance technique [15] (Thermal Microscope, Bethel Co., Ltd., TM3) at 1 MHz. The coefficients of linear thermal expansion of W–Cu–W three-layered films were measured by the thermo mechanical analysis (TMA, Seiko Instruments inc., SS120). The measurement was carried out from 50 to 150 $^{\circ}\text{C}$ at a heating rate of 5 $^{\circ}\text{C min}^{-1}$.

3 Results and discussion

3.1 Characterization of electrodeposited tungsten film

Galvanostatic electrolysis was carried out on a copper substrate at 30 mA cm^{-2} for 40 min in $\text{KF-B}_2\text{O}_3\text{-WO}_3$ melt at 850 $^{\circ}\text{C}$. A silver metallic film was obtained on both sides of the copper substrate after the electrolysis. The appearance and the surface SEM image of the deposit are shown in Fig. 2. No crack or void was observed while the surface looked like an angular face.

Tungsten metal can form two crystal structures, α -phase and β -phase, which was reported to appear in electrodeposition from molten salts [8]. An XRD pattern of the deposit is shown in Fig. 3. All peaks were assigned to α -tungsten. In order to evaluate preferred orientation parallel to a substrate plane, orientation index M was calculated as follows [16],

$$M(hkl) = \frac{\frac{I(hkl)}{\sum I(h'k'l')}}{\frac{I_0(hkl)}{\sum I_0(h'k'l')}} \quad (1)$$

where $I(hkl)$ is XRD intensity in experimental data, $I_0(hkl)$ is the intensity in JCPDS cards and $M(hkl)$ is the calculated orientation index. $\sum I(h'k'l')$ in the present case is the sum of intensities of six peaks: (110), (200), (211), (220), (310), (321). The calculated orientation indices are listed in Table 1. The (222) plane was significantly oriented parallel to the substrate. Concerning the reason why tungsten is electrodeposited successfully from the melt containing B_2O_3 and KF , Koyama et al. [7] proposed the acid–base cooperative reaction as below. B_2O_3 acts as a Lewis acid and F^- acts as a Lewis base. Tungsten oxide is regarded as the salt based on W^{6+} Lewis acid and O^{2-} Lewis base. Since B_2O_3 is a stronger acid than W^{6+} and O^{2-} is a stronger base than F^- , some O^{2-} is extracted from WO_3 by B_2O_3 and alternatively some F^- coordinate to tungsten ion. A probable reaction is:



The formed tungsten oxyfluoride ion can be easily discharged at a cathode to give a smooth electrodeposit of tungsten.

Figure 4 shows an SEM image of the cross-section. It was found that three layers of a W–Cu–W are seen, where the thicknesses of the tungsten and the copper are 13.0 and 20.0 μm , respectively. It is often reported that the electrodeposit from molten salts contains some salts in voids and cracks. So a cross-sectional SEM observation in larger magnification and an EDX analysis were carried out. As shown in Fig. 5, no void or crack was observed. The EDX spectrum of deposit is shown in Fig. 6. Two peaks are ascribed to tungsten, and no element of salts was observed. Thus, it was concluded that the obtained tungsten contained no impurity and had a compact structure. From Fig. 5, it is also seen that the electrodeposited tungsten layer has a unique microstructure. It is composed of relatively fine grains near the substrate, which then changes to the microstructure with much coarser grains at greater distances from the substrate. Such change in microstructure can be explained by the effect of substrate [17]. Nucleation occurs easily on the copper substrate, while nucleus growth proceeds predominantly on the “electrodeposited tungsten”.

To observe the difference in electrodeposition behavior on two different substrates, the linear sweep voltammetry was performed for a copper electrode and an “electrodeposited tungsten” electrode. Thus, as shown in Fig. 7, cathodic currents were observed from 0 V versus W for both electrodes, which should correspond to the electrodeposition of tungsten. Current density was larger for the copper

Fig. 2 An appearance and a surface SEM image of the electrodeposit on a copper substrate obtained at 30 mA cm^{-2} for 40 min from the $\text{KF-B}_2\text{O}_3\text{-WO}_3$ melt at $850 \text{ }^\circ\text{C}$

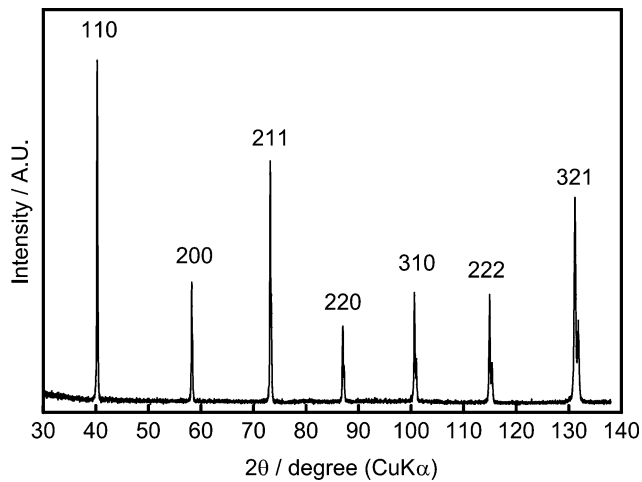
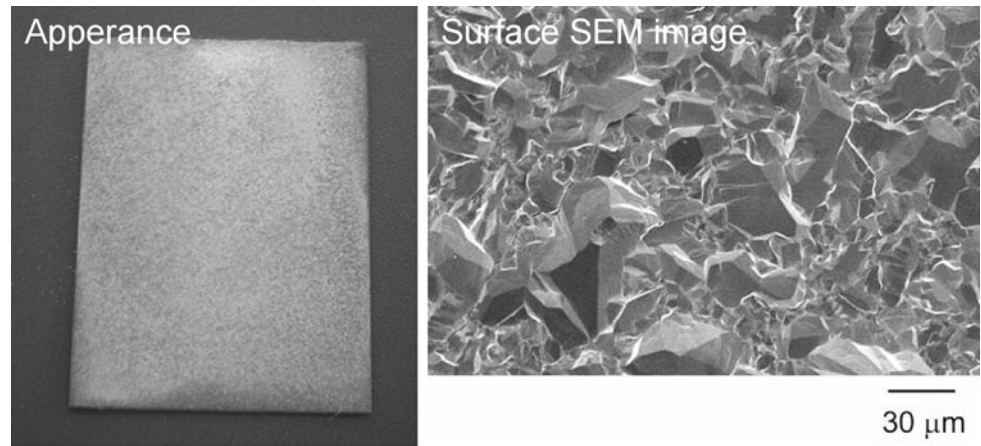


Fig. 3 An XRD pattern of the electrodeposit on a copper substrate obtained at 30 mA cm^{-2} for 40 min from the $\text{KF-B}_2\text{O}_3\text{-WO}_3$ melt at $850 \text{ }^\circ\text{C}$

Table 1 Orientation M of of the electrodeposit on a copper substrate obtained at 30 mA cm^{-2} for 40 min from the $\text{KF-B}_2\text{O}_3\text{-WO}_3$ melt at $850 \text{ }^\circ\text{C}$

Plane	(110)	(200)	(211)	(310)	(222)	(321)
$M(hkl)$	0.52	1.20	1.59	1.50	4.17	1.74

electrode than that for the electrodeposited tungsten electrode. It was confirmed that the overpotential in electrodeposition is larger for the electrodeposited tungsten electrode than for the copper electrode. It can be explained by that the nucleation occurs easily on the copper substrate compared to the electrodeposited tungsten substrate, which is consistent with the above discussion on microstructure.

3.2 Properties of electrodeposited tungsten film

The hardness of electrodeposited tungsten was measured by nano indentation and found to be 8.4 GPa , which was larger than that of monocrystal tungsten reported by Oliver

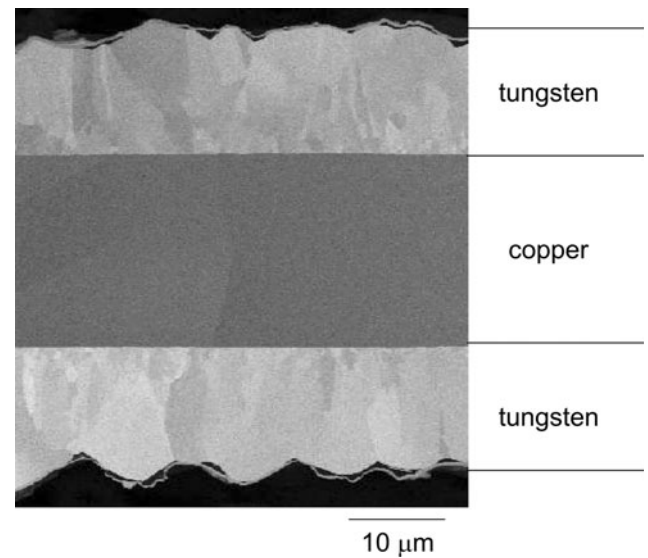


Fig. 4 A cross sectional view of the electrodeposit on a copper substrate obtained at 30 mA cm^{-2} for 40 min from the $\text{KF-B}_2\text{O}_3\text{-WO}_3$ melt at $850 \text{ }^\circ\text{C}$

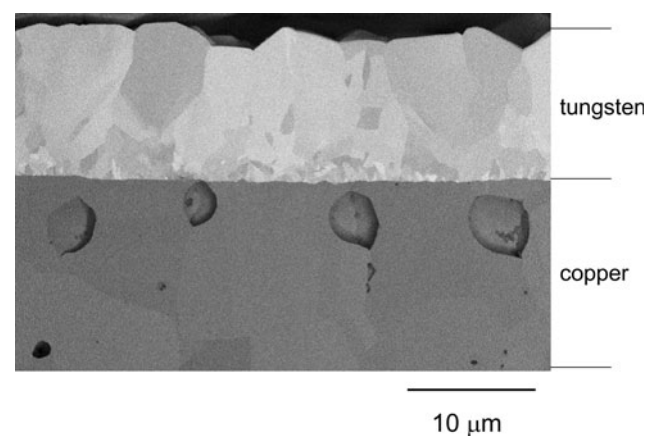


Fig. 5 A cross sectional view of the electrodeposit on a copper substrate obtained at 30 mA cm^{-2} for 40 min from the $\text{KF-B}_2\text{O}_3\text{-WO}_3$ melt at $850 \text{ }^\circ\text{C}$ in larger magnification

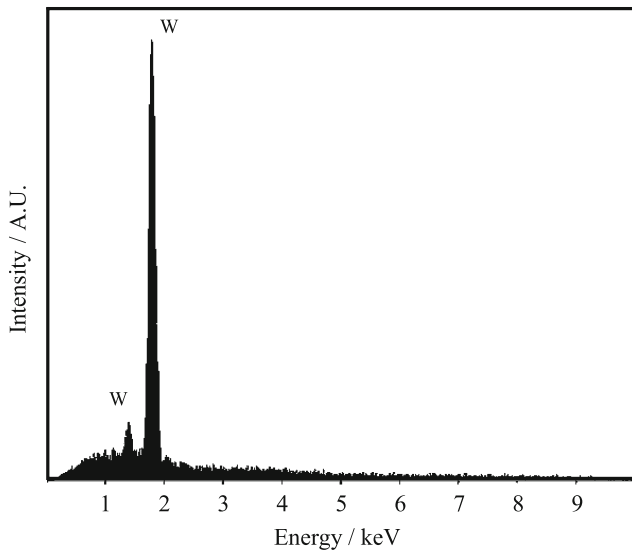


Fig. 6 An EDX spectrum of the electrodeposit on a copper substrate obtained at 30 mA cm^{-2} for 40 min from the $\text{KF-B}_2\text{O}_3\text{-WO}_3$ melt at $850 \text{ }^\circ\text{C}$

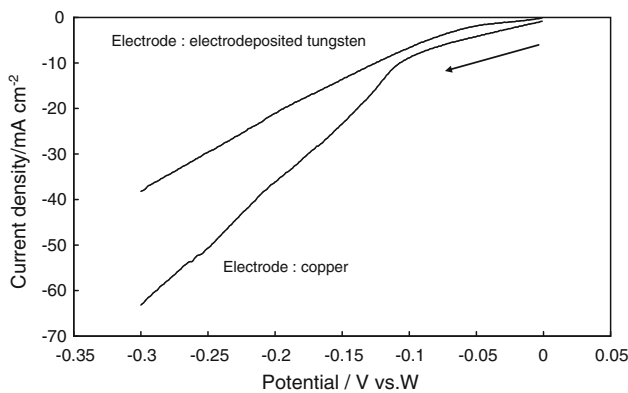


Fig. 7 Linear sweep voltammograms for a copper electrode or an electrodeposited tungsten electrode

et al. [14] (about 5 GPa). The reason of the larger hardness is considered to be due to the small grain size. By nano indentation, Young’s modulus was also measured and found to be 406 GPa. This value was almost the same as the reported value for monocrystal tungsten, which was 410 GPa [18].

After removing a copper substrate by nitric acid solution, the linear thermal expansion of the electrodeposited tungsten was measured by the laser speckle technique. As shown in Fig. 8, the linear thermal expansion was almost proportional to the temperature from 50 to $200 \text{ }^\circ\text{C}$ and its coefficient was $4.5 \times 10^{-6}/\text{K}$. This value was the same as the reported value for the tungsten produced by a conventional method [19].

The relation between a thermal effusivity and a thermal conductivity is expressed by a following equation [15],

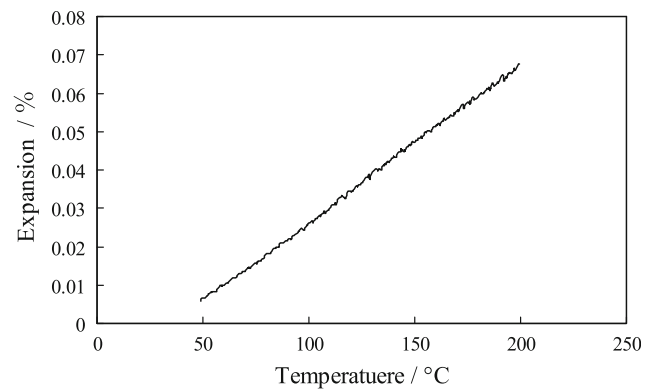


Fig. 8 The linear thermal expansion for the tungsten electrodeposit obtained at 30 mA cm^{-2} for 40 min from the $\text{KF-B}_2\text{O}_3\text{-WO}_3$ melt at $850 \text{ }^\circ\text{C}$

$$b = (\rho C_p \lambda)^{-1/2} \tag{3}$$

where b , ρ , C_p and λ are thermal conductivity, density, specific heat and thermal diffusivity, respectively. Here, λ was measured by the thermoreflectance technique and found to be $2.13 \times 10^4 \text{ J s}^{-1/2} \text{ m}^{-2} \text{ K}^{-1}$. Then the thermal conductivity was calculated to be $178 \text{ W m}^{-1} \text{ K}^{-1}$. This value was near the reported value for the tungsten produced by a conventional method, which was $167 \text{ W m}^{-1} \text{ K}^{-1}$ [20].

3.3 The coefficients of linear thermal expansion of W–Cu–W three-layered films

As shown in Fig. 4, a W–Cu–W three-layered film can be prepared by electrodeposition of tungsten on the both sides of a thin copper film. If the volume ratio of tungsten to copper in such a film can be controlled, it is possible to produce a heat sink material having any desired coefficients of linear thermal expansion. Considering the use for a heat sink, the thermal expansion in the horizontal direction is important. For the W–Cu–W three-layered film, the coefficient of linear thermal expansion in the horizontal direction can be predicted by the theory of composite material as follows,

$$\alpha_{\text{complex}} = \frac{\alpha_w V_w E_w + \alpha_{\text{Cu}} V_{\text{Cu}} E_{\text{Cu}}}{V_w E_w + V_{\text{Cu}} E_{\text{Cu}}} \tag{3}$$

where α_i , V_i and E_i are the coefficient of linear thermal expansion, volume ratio and the Young’s modulus of material i ($i = \text{W}$ or Cu).

For the verification of the possibility of this three-layered film to the heat sink application, two films were produced by electrodepositing tungsten on a copper film at 30 mA cm^{-2} for 20 or 40 min. According to the cross-sectional SEM observations of the films, the V_w of three-layered films were

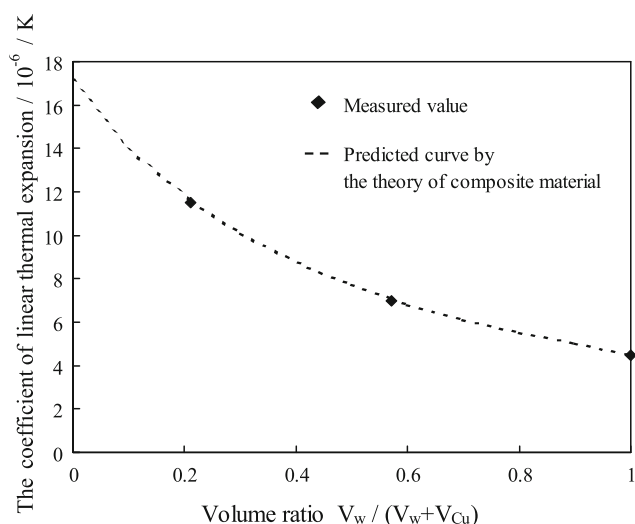


Fig. 9 The coefficients of linear thermal expansion for W–Cu–W three layered films

found to be 0.21(W:Cu:W = 6.7:50.0:6.7, in μm) and 0.57(W:Cu:W = 13.0:20.0:13.0, in μm). Then the coefficients of linear thermal expansion were measured by the thermo mechanical analysis. The results are shown in Fig. 8 with the predicted curve by the Eq. 3. The measured values agree well with the predicted values by the theory of composite material.

So this three-layered film is very promising for the heat sink application, because its coefficient of linear thermal expansion can be controlled easily (Fig. 9).

4 Conclusions

A tungsten film of 13 μm in thickness was obtained on a copper substrate by galvanostatic electrolysis at 30 mA cm^{-2} for 40 min in a $\text{KF-B}_2\text{O}_3\text{-WO}_3$ (67:26:7 mol%) melt at 850 $^\circ\text{C}$. The electrodeposited tungsten did not contain cracks, voids and any elements of the molten salt. The hardness and Young's modulus of the tungsten were found to be 8.4 and 410 GPa by nanoindentation. The coefficient of linear thermal expansion and the thermal conductivity were determined

to be $4.5 \times 10^{-6} \text{ K}^{-1}$ and $178 \text{ W m}^{-1} \text{ K}^{-1}$, which were similar values with the tungsten produced by a conventional powder metallurgy process. Furthermore, a W–Cu–W three-layered film was prepared by tungsten electrodeposition for the heat sink application. The coefficients of linear thermal expansion of the prepared films agreed well with the predicted values by the theory of composite material, which demonstrate the three-layered film is very promising due to the easiness in controlling its coefficient of linear thermal expansion.

References

1. Lin D, Shin M, Zheng F (2008) IEEE Trans Compon Packag Technol 31:196
2. Stewart D, Wilson P (1980) Vacuum 30:527
3. Cadden C, Odegard B Jr (2000) J Nucl Mater 283–287:1253
4. Furutani K, Shibatani K, Itoh N, Mohri N (1998) Precis Eng 22:131
5. Senderoff S, Mellors G (1966) Science 153:1475
6. Senderoff S, Mellors G (1967) J Electrochem Soc 114:586
7. Koyama K, Morishita M, Umezumi T (1999) Electrochemistry 67:667
8. Katagiri A, Suzuki M, Takehara Z (1991) J Electrochem Soc 138:767
9. Masuda M, Takenishi H, Katagiri A (2001) J Electrochem Soc 148:C59
10. Nakajima H, Nohira T, Hagiwara R (2005) Electrochem Solid-State Lett 8:C91
11. Yuen A (2007) Laser Focus World 43(7):83
12. Tsunekane M, Taira T (2007) IEEE J Sel Top Quantum Electron 13:619
13. Kim J, Ryu S, Kim Y, Moon I (1998) Scr Mater 39:669
14. Oliver C, Pharr G (1992) J Mater Res 7:1564
15. Taketoshi N, Ozawa M, Ohta H, Baba T (1999) AIP Conf Proc 463:315
16. Yoshimura S, Yoshihara S, Shirakashi T, Sato E (1994) Electrochim Acta 39:589
17. Paunovic M, Schlesinger M (1998) Fundamentals of electrochemical deposition, Chap. 7. John Wiley and Sons, New York
18. Simmons G, Wang H (1971) Single crystal elastic constants and calculated aggregate properties: a handbook, 2nd edn. The M.I.T. Press, Cambridge
19. Gurneyuk V, Lebedev V (1961) Fiz Metall 11:29
20. Smithells C (1952) Tungsten. Chapman and Hall, London